

An Explanation for Non-Power-law Behavior in the Hard X-ray Spectrum of the July 23, 2002 Solar Flare

Eduard P. Kontar¹, John C. Brown^{1,2}, A. Gordon Emslie², Richard A. Schwartz³,
David M. Smith⁴, & R. Calum Alexander¹

ABSTRACT

High-resolution RHESSI data reveal that solar flare hard X-ray spectra show systematic deviations from power-law behavior. Even for injection of a power-law electron spectrum, such deviations are expected because of a number of effects, including nonuniform target ionization and solar albedo backscattering of the primary hard X-ray flux. In this paper we examine 1 keV resolution hard X-ray spectra for the intense July 23, 2002 event, corrected for the effects of decimation, pulse pile-up and background. We find that the observed spectra indeed deviate from a power-law behavior in a manner consistent with the effects of nonuniform target ionization. Further, this interpretation of the observed deviations requires that the amount of coronal material increases during the initial phase of the flare. The implications of this discovery for models of atmospheric response to flare heating are discussed.

Subject headings: Sun: flares, X-rays, Sun: transition region

1. Introduction

Solar flare hard X-ray spectra may contain non-power law features, i.e., changes in the local power-law spectral index $\gamma(\epsilon)$ (e.g., Johns & Lin 1992; Thompson et al. 1992; Piana,

¹Department of Physics & Astronomy, The University, Glasgow G12 8QQ, UK
eduard@astro.gla.ac.uk, john@astro.gla.ac.uk, calum@astro.gla.ac.uk

²Department of Physics, The University of Alabama in Huntsville, Huntsville, AL 35899
emslieg@uah.edu

³SSAI, Laboratory for Astronomy and Solar Physics, Code 682, NASA Goddard Space Flight Center, Greenbelt, MD 20771
richard.schwartz@gssc.nasa.gov

⁴Space Sciences Laboratory, University of California at Berkeley, Berkeley, CA 94720, USA
dsmith@ssl.berkeley.edu

Brown & Thompson 1995). It is tempting to attribute such features to corresponding features in the accelerated electron distribution. However, there are important physical processes that produce non-power-law photon spectra even if the injected electron spectrum is a power law. Amongst these processes are (1) photospheric albedo (Hénoux 1975; Langer & Petrosian 1977; Bai & Ramaty 1978; Alexander & Brown 2002), which produces an enhancement in the 30-100 keV range and (2) non-uniform ionization of the flare target (Brown 1973a, Brown et al. 1998), which produces a local spectral hardening around photon energy $\epsilon = E_*$, the minimum electron energy required to reach the near-neutral chromospheric layers of the flare (Kontar, Brown, & McArthur 2002; Brown, Emslie & Kontar 2003). In this paper we present evidence for the latter feature in the RHESSI high-resolution photon spectra for the intense July 23, 2002 solar flare. We also discuss the evolution of E_* with time and the implications for models of atmospheric response to flare heating.

2. Data Reduction and Analysis

The unprecedented sensitivity and spectral resolution of RHESSI produces very high-quality count rate spectra. However, it also creates several instrumental issues (see Smith et al. 2002) that must be addressed in the deduction of the corresponding photon spectra, which we now discuss.

First, to conserve onboard memory space during the recording of large events, the count rate is “decimated,” a procedure wherein only 1 out of every N counts (where N is a variable, but known, number) is actually recorded. Allowance for decimation to reproduce actual count spectra is straightforward.

Second, the onboard electronics requires a finite time ($\simeq 8 \times 10^{-7}$ s) to detect a photon event. Multiple photons that arrive at a detector within this interval are therefore recorded as a single count with an energy equal to the sum of the individual photons involved. This “pulse pileup” effect can be substantial for intense flares such as the July 23 event and must be corrected for (Smith et al. 2002). The number of events wrongly recorded due to pileup is proportional to the square of the observed count rate. This is a function of time due not only to temporal variation in the flare itself, but also to modulation of the incoming flux by the rotating grids.

Use of discrete time intervals and corresponding average count rates generally leads to an underestimation of the pile-up correction. To see this, divide a given time interval into n equal subintervals, with C_i counts in each subinterval. Then the average count rate for the interval is $\langle C \rangle = \sum C_i/n$ and the applied pile-up correction would be $\sim \langle C \rangle^2$.

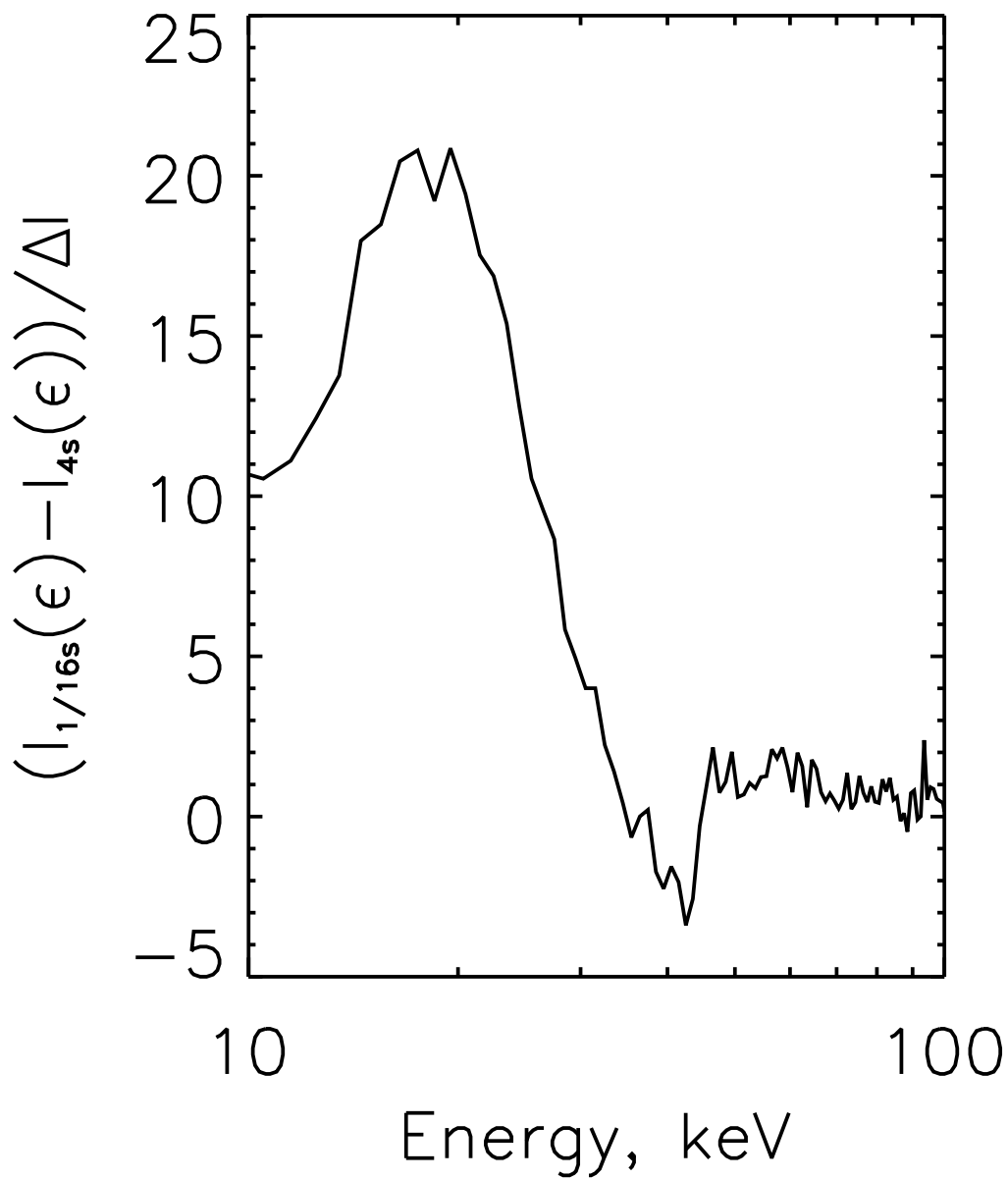


Fig. 1.— Difference (normalized to the statistical error in the data points) between the RHESSI detector # 9 spectrum corrected for pileup with a 0.0625s accumulation interval and that with 4s accumulation interval, for the time interval 00:30:00-00:30:20 UT.

However, the *correct* pile-up correction is $\sim \langle C^2 \rangle$, which is always greater than $\langle C \rangle^2$ (since, because of modulation by the imaging grids, the C_i are never equal, even for a constant source with negligible statistical noise). For a given photon energy, RHESSI's finer grids produce a relatively small modulation amplitude but a relatively high modulation frequency. Conversely, the coarser grids result in a high modulation amplitude (i.e., large variation in C) at a relatively low frequency. Figure 1 compares the spectra corrected for pileup with various time binnings for the detector corresponding to the coarsest grid (# 9); significant spectral features in the energy range below 50 keV are caused by pulse pileup. The error introduced by using time-averaged pileup can be up to 20 times the statistical error in the case of the July 23, 2002 flare.

Third, the detector response in a matrix form must be used to convert count rates to photon fluxes. During periods of intense count rate, the instrument deploys additional attenuator plates in the photon path. The response matrix (Smith et al. 2002) takes into account the presence of these attenuators, along with Compton scattering, K-shell fluorescent escape from the detector surface, attenuation in materials within the cryostat, resolution broadening, and the photoelectric effect. We are confident in our modeling of these effects, even with the full attenuation deployed, at energies above 15 keV.

Fourth, the background must in general be accurately evaluated and subtracted to obtain the true solar photon spectrum. However, for the intense July 23 event, the exact determination of the (relatively weak) background flux is not crucial to the analysis.

For our analysis we used 1 keV binned data collected over 20 second time intervals from 00:27:00 - 00:38:00 UT and corrected for decimation, pileup, detector response and background. The spectra were summed over 7 front segment detectors from detectors 1 through 9, excluding detectors #2 and #7 due to their limited energy resolution. The data was processed using Release Version 8 of the RHESSI Software and the SPEX software available on the Solar Software Tree.

3. Spectral Features Associated with Nonuniform Target Ionization

As shown by Kontar, Brown, & McArthur (2002), a power-law electron spectrum injected from a coronal source toward a neutral chromosphere produces (for Kramers' cross-section) a photon spectrum

$$I(\epsilon) = \frac{I_0}{(\lambda + 1)\epsilon} \left[\frac{\epsilon^{2-\delta}}{\delta - 2} + \frac{E_*^{2-\delta}}{2\lambda} B \left(\frac{1}{1 + (\epsilon/E_*)^2}, \frac{\delta}{2} - 1, \frac{1}{2} \right) \right], \quad (1)$$

where $\lambda = 0.55$ is a factor related to the ratio of collisional energy loss cross-sections in ionized and neutral targets, I_0 is an electron flux scale factor, δ is the spectral index of the injected electron spectrum, $B(x; a, b)$ is the incomplete beta function and E_* (keV) $\simeq \sqrt{10^{-17} N_*}$ is the minimum electron energy required to reach the chromospheric layers at column density N_* (cm^{-2}), where the ionization fraction of the ambient target drops sharply below unity. (We recognise that the Kramers cross-section, and hence the form [1], is only a first approximation but believe it is adequate for the present purpose, namely a comparison of the goodness of different model fits.)

For $E_* \rightarrow 0$ or $E_* \rightarrow \infty$, $I(\epsilon)$ assumes the power-law form $I(\epsilon) \sim \epsilon^{-\gamma}$, with $\gamma = \delta - 1$. However, for $\epsilon \simeq E_*$, the spectrum (1) flattens, with a local power-law slope $\gamma < \delta - 1$ (cf. Brown, Emslie, & Kontar 2003). We therefore seek evidence for such local spectral flattenings, and the corresponding values of E_* , for the photon spectra observed in the July 23, 2002 event.

Following Holman et al. (2003), we first fit the photon spectra obtained in §2 to the sum of a thermal Maxwellian at a single temperature T plus a power-law of index γ . We here limit ourselves to the issue of deviations from a power law in the “nonthermal” component of the spectrum above ~ 40 keV. The upper panel of Figure 2 shows an example of such deviations, which represent significant deviations from the power-law fit at energies above ~ 40 keV. These deviations are much reduced by replacing the power-law by expression (1), with the minimum rms residual obtained for values of $\delta = 4.24$ and $E_* = 53$ keV (lower panel of Figure 2). The χ^2 for the fit over the 10 – 300 keV range is 0.8, compared to the χ^2 for a thermal-plus-power-law fit of 1.4. There are still significant residuals present in the range from $\sim 10 - 30$ keV; these are most probably due to the assumption of a single temperature thermal component. Consideration of additional thermal emission from plasma at temperatures in the range $\sim 3 - 10$ keV should account for these residuals (Piana et al. 2003), but will not significantly affect the spectrum at energies above ~ 40 keV and so the conclusions of this paper.

4. Temporal Variations of the Fit Parameters

Allowance for nonuniform target ionization offers an elegant direct explanation for the shape of the observed hard X-ray spectrum. It also allows the values of the fit parameters kT (keV), δ and E_* to be estimated as functions of time, as shown in Figure 3, together with the corresponding value of $N_*(\text{cm}^{-2}) \simeq 10^{17} E_*(\text{keV})^2$.

The thermal plasma temperature rises quickly to a value $\simeq 3$ keV and decreases fairly

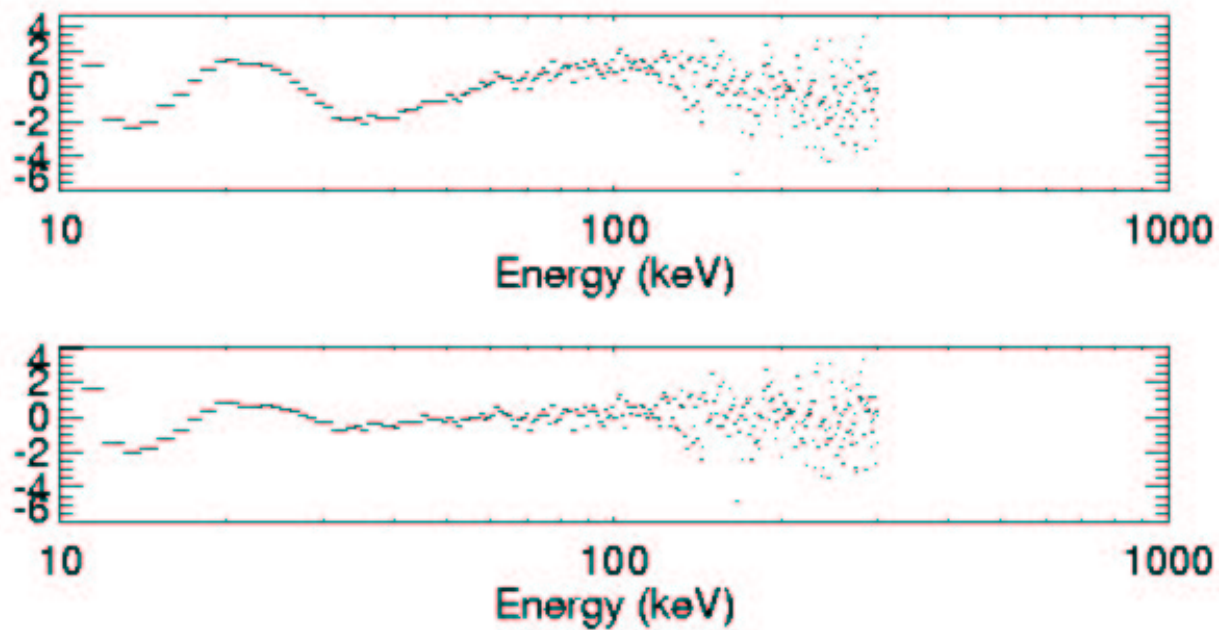


Fig. 2.— Photon spectrum residuals, normalized by the statistical error for the spectral fit, for the time interval 00:30:00 - 00:30:20 UT for (upper panel) an isothermal Maxwellian plus power-law and (lower panel) an isothermal Maxwellian plus the nonuniform ionization spectrum given by Equation (1) with $\delta = 4.24$ and $E_* = 53$ keV.

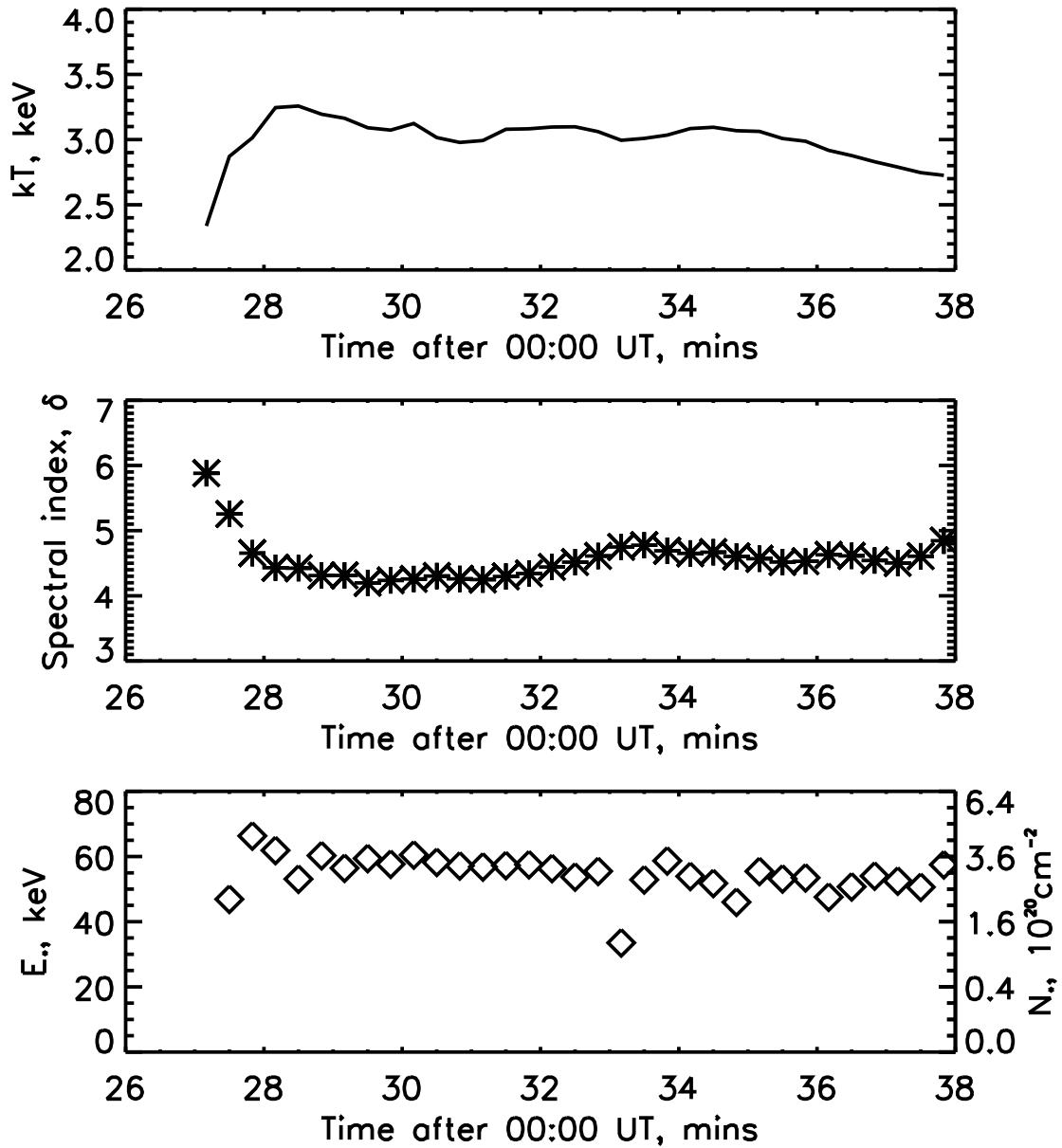


Fig. 3.— Variation of kT , δ , E_* , and N_* throughout the event. The variation of other parameters, such as emission measure, can be found in Holman et al. (2003).

slowly thereafter. The injected electron flux spectral index δ follows a general “soft-hard-soft” trend (Fletcher & Hudson 2002) and qualitatively agrees with the time history of the simple best-fit power-law index γ (Holman et al. 2003). E_* rises quickly during the first minute or so from ~ 40 keV to ~ 70 keV near the flare peak and thereafter declines rather slowly. The corresponding values of N_* are $\sim 2 \times 10^{20} \text{ cm}^{-2} - 5 \times 10^{20} \text{ cm}^{-2}$.

5. Discussion and Conclusions

The essential results of this study are that (1) for a power-law electron injection spectrum, the expression for bremsstrahlung emission from a nonuniformly-ionized target is a better fit to observed spectra than the expression for a uniform target for energies above 40 keV; and (2) the value of E_* (and correspondingly N_*) varies with time.

The time for the increase in E_* to occur is of order a minute, much larger than the timescale to reach ionization equilibrium at the relevant number densities $n \sim 10^{12} \text{ cm}^{-3}$, yet consistent with hydrodynamic timescales (\sim scale height/sound speed) for coronal density increase due to chromospheric evaporation in impulsive electron-heated scenarios (e.g., Mariska, Emslie, & Li 1989). For the event in question, however, this timescale is also comparable to the rise time in the injected electron flux (see lightcurves in Holman et al. 2003). In such cases, the atmosphere evolves through a series of quasistatic density profiles; the amount of coronal material being dependent on the instantaneous electron flux (e.g., Brown 1973c). In a closed loop the increase in N_* creates a growing coronal overpressure which in turn causes the rate of chromospheric evaporation to drop *below* the injected electron flux profile (and so the hard X-ray intensity; Brown et al. 2000). Figure 3 shows some evidence for just such a gradual decline in E_* from 00:28 UT to 00:38 UT.

It is of interest to consider also the absolute values of E_* and N_* from a theoretical point of view. N_* can be roughly defined as the depth at which the hydrogen ionization fraction x falls to 0.5. While this can occur over a wide range of densities, depending on the flare model adopted, the temperature at this level is always close to $T_x \simeq 8500$ K (e.g., Brown 1973b; Machado et al. 1980). For empirical models of large flares (e.g., model F2 of Machado et al. 1980), appropriate to the July 23, 2002 event, this temperature occurs at $N_* \simeq 1 \times 10^{19} \text{ cm}^{-2}$.

This value of N_* can be compared with the value of N_{tr} , the column density at the top of the radiatively stable chromosphere, where the temperature is equal to the peak in the optically thin radiative loss curve $f_{\text{rad}}(T)$, viz. $T = T_c \simeq 60,000$ K (e.g., Raymond et al. 1976). Neglecting ambient heating and assuming ionization equilibrium (see above), the

variation of temperature with depth in a beam-heated chromosphere is obtained by balancing beam heating ($\sim n\mathcal{F}_{20}N^{-\delta/2}$) and radiative cooling ($= n^2 f_{rad}[T]$), where n is the local number density (cm^{-3}) and \mathcal{F}_{20} is the electron energy flux ($\text{erg cm}^{-2} \text{ s}^{-1}$ above [arbitrary] reference energy $E = 20 \text{ keV}$). Hydrostatic pressure balance requires that $nT \sim N$, so that setting $f_{rad} \sim T^3$ (Raymond et al. 1976), the energy balance relation becomes

$$N \sim \mathcal{F}_{\delta+2}^{2/\delta+2} T^{-4/\delta+2}. \quad (2)$$

With $\delta = 4$ (see Figure 3), we obtain

$$\frac{N_*}{N_{\text{tr}}} = \left(\frac{8,500}{60,000} \right)^{-\frac{2}{3}} \simeq 3.7; \quad \frac{E_*}{E_{\text{tr}}} \simeq 1.9, \quad (3)$$

where E_{tr} is the energy required to reach depth N_{tr} . The absolute value of N_{tr} is obtained by setting $T = T_c$ in Equation (2) and applying the scale factor from Equation [7] of Doyle et al. (1985, correcting errors in Brown 1973c). For $\delta = 4$ this gives

$$N_{\text{tr}} = 3.3 \times 10^{18} T_1^{\frac{1}{3}} \left(\frac{\mathcal{F}_{20}}{10^{11}} \right)^{\frac{1}{3}}, \quad (4)$$

The quantity T_1 appears in the above through the hydrostatic relation between the gas pressure $2nkT_1$ and the overlying column weight $\simeq N_{\text{tr}}m_Hg$ (where k is Boltzmann’s constant, m_H the hydrogen mass and g the solar gravity); its value depends on whether the flare heated matter has yet expanded to a new hydrostatic state. There are two extreme cases. In the first, considered by Doyle et al. (1985), the heating is so impulsive that T_1 reflects the temperature (and so the scale height) of the preheated chromosphere, viz. $T_1 \simeq 5000 \text{ K}$. In the other extreme (Brown 1973c), the heating is considered quasi-steady, so that the chromosphere maintains a hydrostatic (open-top) loop equilibrium. In this case, the appropriate value of T_1 is $T_1 = T_c \simeq 60,000 \text{ K}$. The gradual rise in hard X-ray flux for the July 23, 2002 event implies that the latter case is more appropriate, so that

$$N_{\text{tr}} = 1.3 \times 10^{20} \left(\frac{\mathcal{F}_{20}}{10^{11}} \right)^{\frac{1}{3}}; \quad E_{\text{tr}} (\text{keV}) = 32 \left(\frac{\mathcal{F}_{20}}{10^{11}} \right)^{\frac{1}{6}}. \quad (5)$$

By Equation (3), the corresponding values of N_* and E_* are,

$$N_* = 4.9 \times 10^{20} \left(\frac{\mathcal{F}_{20}}{10^{11}} \right)^{\frac{1}{3}}; \quad E_* (\text{keV}) = 62 \left(\frac{\mathcal{F}_{20}}{10^{11}} \right)^{\frac{1}{6}}; \quad (6)$$

or somewhat lower if allowance is made for the effects of overpressure in a closed flux tube (Brown et al. 2000).

Note that these are relatively weak scalings with \mathcal{F}_{20} . Even for an order of magnitude increase in \mathcal{F}_{20} over the main phase of the flare (see Holman et al. 2003), E_* increases by only a factor of $10^{1/6} \simeq 1.5$. The value of E_* in Equation (6) agrees with the values in Figure 3 for $\mathcal{F}_{20} \simeq 10^{11}$ erg cm⁻² s⁻¹.

Holman et al. (2003) estimate, from the spatially-integrated hard X-ray flux, that the peak injected power $P_{20} \simeq 10^{29}$ erg s⁻¹; a beam energy flux $\mathcal{F}_{20} \simeq 10^{11}$ erg cm⁻² s⁻¹ thus corresponds to a beam area $\simeq 10^{18}$ cm². This is comparable to the footpoint area found through hard X-ray imaging for this event (Emslie et al. 2003).

In addition to the correction for target ionization structure, the hard X-ray spectrum is modified by the photospheric albedo contribution, mainly in the 30-60 keV energy range and serendipitously in the same range as the values of E_* found above. Using the Bai & Ramaty (1978) results, we have found (Alexander et al. 2003) that adding albedo corrections alone to a pure power-law spectrum reduces the χ^2 of the fit from 1.4 to 0.8, while combining the albedo and nonuniform target ionization factors reduces it somewhat further (to 0.6). We conclude that the data are consistent with the presence of *both* effects, although a detailed comparison will require more work on albedo modelling, taking into account the effect of flare heliocentric distance and relaxing some of the more restrictive model assumptions used to date (e.g., Bai & Ramaty 1978), such as the geometry of the primary hard X-ray source and the angular distribution of the primary photon distribution.

As a final remark, our analysis here has been based entirely on a power-law electron injection spectrum. However, even for other injected spectral forms, the effect of ionization structure would introduce comparable features in the photon spectrum at energies $\simeq E_*$. In other words, incorporation of non-uniform ionization structure is clearly a key factor to be considered in the reconstruction *any* observed photon spectrum due to a thick target beam.

This work was supported by NASA’s Office of Space Science and by a PPARC RHESSI Mission Grant.

REFERENCES

- Alexander, R. C., & Brown, J.C. 2002, Sol. Phys., 210, 407
 Alexander, R. C., Kontar, E. P., Brown, J. C., & Emslie, A. G. 2003, in preparation

- Bai, T., & Ramaty, R. 1978, *ApJ*, 219, 705
- Brown, J.C. 1973a, *Sol. Phys.*, 28, 151
- Brown, J.C. 1973b, *Sol. Phys.*, 29, 421
- Brown, J.C. 1973c, *Sol. Phys.*, 31, 143
- Brown, J.C., Emslie, A.G., & Kontar, E.P. 2003, *ApJ*, this volume
- Brown, J.C., Krucker, S., Güdel, M., & Benz, A.O. 2000, *A&A*, 359, 1185
- Brown, J.C., McArthur, G.K., Barrett, R.K., McIntosh, S.W., & Emslie, A.G. 1998, *Sol. Phys.*, 179, 379
- Doyle, J.G., Byrne, P.B., Dennis, B.R., Emslie, A.G., Poland, A.I., & Simnett, G.M. 1985, *Sol. Phys.*, 98, 141
- Emslie, A.G., Kontar, E.P., Krucker, S., & Lin, R.P. 2003, *ApJ*, this volume
- Fletcher, L. & Hudson, H.S. 2002, *Sol. Phys.*, 210, 307
- Hénoux, J.-C. 1975, *Sol. Phys.*, 42, 219
- Holman, G.D., Sui, L., Schwartz, R.A., & Emslie, A.G. 2003, *ApJ*, this volume
- Johns, C., & Lin, R.P. 1992, *Sol. Phys.*, 137, 121
- Kontar, E.P., Brown, J.C., & McArthur, G.K. 2002, *Sol. Phys.*, 210, 419
- Langer, S.H., & Petrosian, V. 1977, *ApJ*, 215, 666
- Machado, M.E., Avrett, E.H., Vernazza, J.E., & Noyes, R.W. 1980, *ApJ*, 242, 336
- Mariska, J.T., Emslie, A.G. & Li, P. 1989, *ApJ*, 341, 1067
- McClymont, A.N., & Canfield, R.C. 1986, *ApJ*, 305, 936
- Piana, M., Brown, J.C, and Thompson A.M. 1995, *Sol. Phys.*, 156, 315
- Piana, M., Massone, A., Kontar, E.P., Emslie, A.G., Brown, J.C., & Schwartz, R.A. 2003, *ApJ*, this volume
- Raymond, J.C., Cox, D.P., & Smith, B.W. 1976 *ApJ*, 204, 290
- Smith, D. M., and 19 co-authors 2002, *Sol. Phys.*, 210, 33
- Thompson A.M., Brown J.C., Craig, I.J.D., & Fulber, C. 1992, *A&A*, 265, 278